Bioethanol-Aided Electrolysis of H_2O

ECS Transactions, 111 (6) 1195-1202 (2023)
10.1149/11106.1195ecst ©The Electrochemical Society

Bioethanol-Aided Electrolysis of H_2O

M. Lo Faro[a], F. Berto Ometto[b], J. Perez[b], and E. Ticianelli[b]

[a] Institute of Advanced Energy Technologies (ITAE) of the Italian National Research Council (CNR), Via Salita S. Lucia sopra Contesse 5, 98126 Messina, Italy
[b] Instituto de Quimica de São Carlos - USP, Av. Trab. São-carlense, 400, Brazil

This manuscript describes a novel electrochemical process for the electrochemical production of H_2 using a solid oxide electrochemical cell. Part of the energy required for the process was supplied by ethanol, which was oxidized at the anode of a fully perovskite cell. In this experiment, we used a tailored cobaltite for the electrodes and a gallate-based perovskite electrolyte ($La_{0.9}Sr_{0.1}Ga_{0.8}Mg_{0.2}O_{3-\delta}$ − LSGM) as the supporting element of an electrolyte-supporting cell (ESC). The present manuscript presents preliminary results from tests concerning LSGM structural analysis to demonstrate its robustness to reducing atmospheres, electrochemical experiments carried out in a complete cell between 700 °C and 800 °C, and surface analysis of the electrodes. With current densities over 1 A cm^{-2} and voltages between 0.27 and 0.41 V, this electrochemical process demonstrates a viable method for producing green hydrogen.

Introduction

As the world has become increasingly urbanized, the production of greenhouse gases and fine particulates into the atmosphere has resulted in severe health and environmental problems. There is a significant impact on climate change from the transportation sector, which is responsible for roughly 73% of global emissions of carbon dioxide, methane, and nitrogen oxide (1). A solution to these problems involves developing high-efficiency technologies that minimize greenhouse gas emissions during the conversion of energy(2). For this challenge, also choosing the best energy vector could also be crucial. As one of several chemical energy carriers, hydrogen is the most promising because its release of power energy produces pure water. If anything, the problem lies in the process of producing it, from what sources, and using which technology. As of today, H_2 is primarily produced through fossil fuel reforming or through the pyrolysis of biomass. In contrast, water electrolysis is a more reliable technology, especially when it is coupled with renewable energy sources like solar, wind, or biomass. An interesting option in this regard is the use of solid oxide water electrolyzers (SOEC)(3), which are already commercially available as reverse SOFCs. By using a conventional SOEC, H_2O is supplied to the cathode side, where it is reduced to produce H_2 and oxide ions. These ions migrate through the solid electrolyte to recombine at the anode to form oxygen molecules:

Cathode: $2\,H_2O + 4\,e^- \rightarrow 2\,H_2 + 2\,O^=$ (reaction 1)

Anode: $2\,O^= \rightarrow O_2 + 4\,e^-$ (reaction 2)

To generate H_2 at a practical rate, this process usually requires voltages appreciably higher than 1 V(4). Traditionally, these systems use solar, wind, or hydroelectric energy

to generate green hydrogen. Solid oxide electrochemical devices are ideal for this process since they can convert C-based molecules into fuels, for example, CO_2 into methane during electrolysis mode operation(5), or electricity during fuel cell mode operation(6). In the present study, the main idea is to replace the conventional anodic reaction (reaction 1) with biofuel oxidation, specifically bioethanol.

As a result, the ideal anodic reaction is as follows:

Anode: $C_2H_6O + 6O^{=} \rightarrow 2\,CO_2 + 3\,H_2O + 12\,e^{-}$ (reaction 3)

Therefore, by coupling the oxidation of ethanol of reaction 3, this supply partially the energy required by the cathodic reaction of H_2O reduction. Consequently, the H_2 generation can occur with sensibly lower electric energy consumption compared to an usual water electrolyzer (7) and can be considered still as "green" since a renewable bioresource was used(8). The most commonly used support in conventional SOFCs and SOECs is Ni, which under SOEC conditions requires H_2 to avoid extensive reoxidation(9). Often, commercial cells use perovskites as the counter electrode, which are capable of reducing/evolving oxygen, but they are not suitable for oxidizing organic fuels. This paper presents a fully electrochemical symmetrical cell design based on advanced perovskites. $La_{0.9}Sr_{0.1}Ga_{0.8}Mg_{0.2}O_{3-\delta}$ (LSGM) was proposed as an electrolyte, which is considered one of the most promising electrolytes for operation at intermediate temperatures. A Ni-modified perovskite (*i.e.* $La_{1.5}Sr_{1.5}Co_{1.5}Ni_{0.5}O_{7\pm\delta}$ – LSCN) was proposed as electrodes due to its reversible behavior under the most common operating conditions of an electrochemical cell.

Experimental

An LSGM electrolyte pellet was made with Praxair powder. In order to determine this material's reliability under reducing conditions, it was thoroughly investigated preventively. With ALTAMIRA AMI-300 equipment, we conducted a TPR analysis up to 1050 °C in 10% of H_2. Following this analysis, material as-reduced was analyzed using XRD. The powders were ball milled with 2 % butvar for 12 hours in ethanol to minimize friction between powders and jar, then dried and pelletized. Following this, calcination was performed at 1450 °C for 6 hours. By using this procedure, we were able to achieve a pellet with a thickness of 300 microns and a density of 98%. In a sacrificial pellet, densification was analyzed using SEM. Electrochemical tests were conducted on a similar pellet to determine its conductivity.

In parallel, LSCN catalyst was prepared by the Pechini method (citrate complexation route) using stoichiometric amounts of nitrate salts(10). In a subsequent step, the gel obtained using this method was calcined for twelve hours at 1300°C. For the final electrocatalyst, powders of the as-calcined LSCN (70 wt.%) were ground together with 30 wt.% of commercial gadolinia-doped ceria (*i.e.* $Ce_{0.9}Gd_{0.1}O_2$) in a ball mill for 6 h with ethanol to minimize friction. We selected 10% gadolinia-doped ceria for its excellent oxygen storage capacity and reasonable electrical conductivity.

The next step was manufacturing the complete cell and testing it electrochemically. Both sides of the LSGM pellet were coated with the LSCN-CGO electrocatalyst by spray coating and then treated at 1300 °C to achieve good adhesion between the layers and reasonable electrode-electrolyte interfaces. Figure 1 shows a schematic representation of the fully perovskite symmetrical cell investigated. Likewise, the reactions involved in each electrode are schematized in this figure.

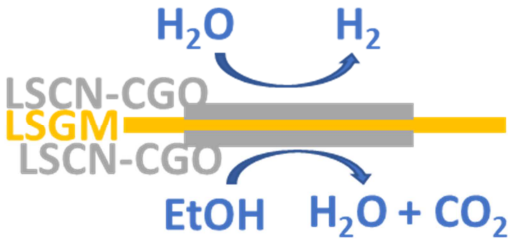

Figure 1. Schematic of the electrochemical cell

The two electrodes of the cell were coated with gold paste, and four gold wires were connected, two on each side, for measuring voltage and current through external electrochemical equipment. The cell was mounted on alumina tubes, sealed on both electrode sides to create a high partial pressure atmosphere for water at the cathode and dry ethanol at the anode, and to prevent gas leakage. A ceramic paste made by AREMCO 316 was used for the cell sealing. A saturated humidified Ar (50cc min^{-1}) was fed to the cathode, while absolute ethanol (99.8%) and Ar (20cc min^{-1}) as carrier were fed to the anode.

Electrochemical characterization included impedance spectroscopy, polarization analyses, and galvanostatic durability tests carried out in the temperature range 700-800 °C. The post-mortem analysis consisted of XPS analyses carried out on the cell using a Physical Electronics (PHI) 5800-01 spectrometer with a monochromatic Al Kα X-ray source (XPS); XRD analyses were measured with a Bruker D8 ADVANCE diffractometer with Cu Kα radiation while the morphology of the spent cell was analyzed with an FEI XL 30 SEM. An overview of this in-depth analysis and its findings is presented in this proceeding.

Results and discussion

A preliminary study was conducted in order to assess the reliability of LSGM for the specific applications suggested in this work. For this purpose, we evaluated the stability of the LSGM structure when exposed to a reducing environment up to 1050°C. In the inset of figure 2, the TPR profile showed a material with limited H_2 consumption starting at 500 degrees Celsius. However, the XRD analyses in figure 2 indicate that the reducing treatment had no significant impact on LSGM's structure. A few more signals were observed in the reduced LSGM compared to the fresh powders purchased from Praxair as a result of the residuals of quartz wool used on each side of the LSGM in order to prevent physical transport of the LSGM in the TPR reactor.

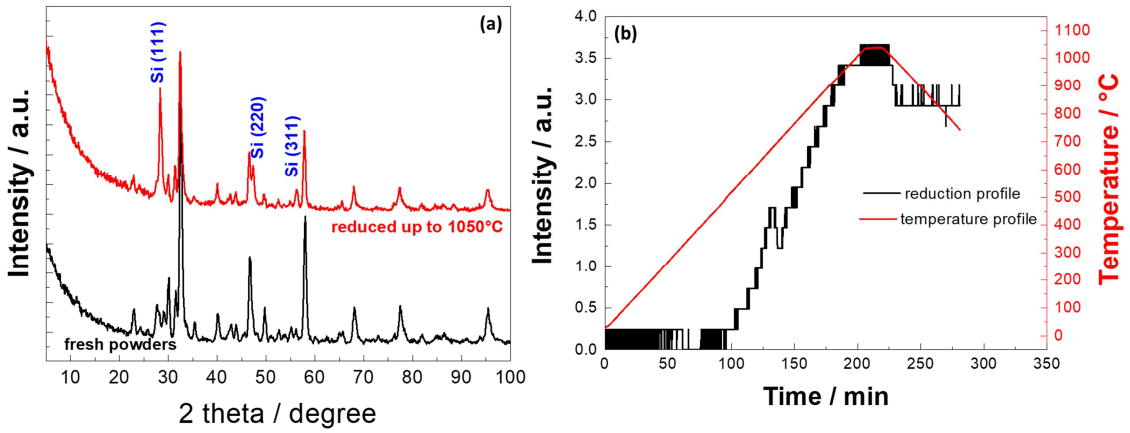

Figure 2. A comparison of the XRD spectra of fresh powder purchased from PRAXAIR and after reduction at 1050°C(a) and TPR profile after thermal treatment with 10 vol. % H_2 in He (b).

This study used LSGM as an electrolyte. In some of our previous papers, we have examined the potentials and behavior of this electrolyte. According to the Arrhenius plot, LSGM had conductivity and activation energy similar to those reported for CGO(11). Even so, the advantage of using LSGM over CGO lies in the fact that it lacks a redox mechanism at least up to 1.4 eV, because above that gallium can be reduced (12). This represents an advantage because a redox mechanism occurring at low potentials results in a partial internal short circuit. The LSGM, however, has limitations on the materials that can be coupled. For instance, its reactivity with Ni at high temperatures is well known. As a result, we designed a fully perovskite cell for this experiment (13).

An initial galvanostatic test using 800 mA cm^{-2} s(Figure 3) showed that the cell potential was 350 mV at 700 °C, although the cell was quite noisy, probably due to cycles of the pump feeding ethanol to the anode. Noise may also be generated by ethanol oxidation, which in general requires many steps according to the following reactions that contribute energetically to the reduction of H_2O at the cathode:

$$CH_3CH_2OH + O^{=} \rightarrow CH_3CHO + H_2O + 2\,e^{-} \quad (E° \approx 1.284 \text{ eV @ } 800 °C) \qquad \text{(reaction 4)}$$

$$CH_3CHO + O^{=} \rightarrow CH_4 + CO_2 + 2\,e^{-} \quad (E° \approx 1.749 \text{ eV @ } 800 °C) \qquad \text{(reaction 5)}$$

$$CH_4 + 2O^{=} \rightarrow CH_2O + H_2O + 4\,e^{-} \quad (E° \approx 0.781 \text{ eV @ } 800 °C) \qquad \text{(reaction 6)}$$

$$CH_2O + O^{=} \rightarrow CO + H_2O + 2\,e^{-} \quad (E° \approx 1.605 \text{ eV @ } 800 °C) \qquad \text{(reaction 7)}$$

$$CO + O^{=} \rightarrow CO_2 + 2\,e^{-} \quad (E° \approx 0.982 \text{ eV @ } 800 °C) \qquad \text{(reaction 8)}$$

After 15 hours of working and being placed at 800 °C, some improvement was seen in this behavior. During this period, the cell's average potential was 220 mV, as seen in Figure 3.

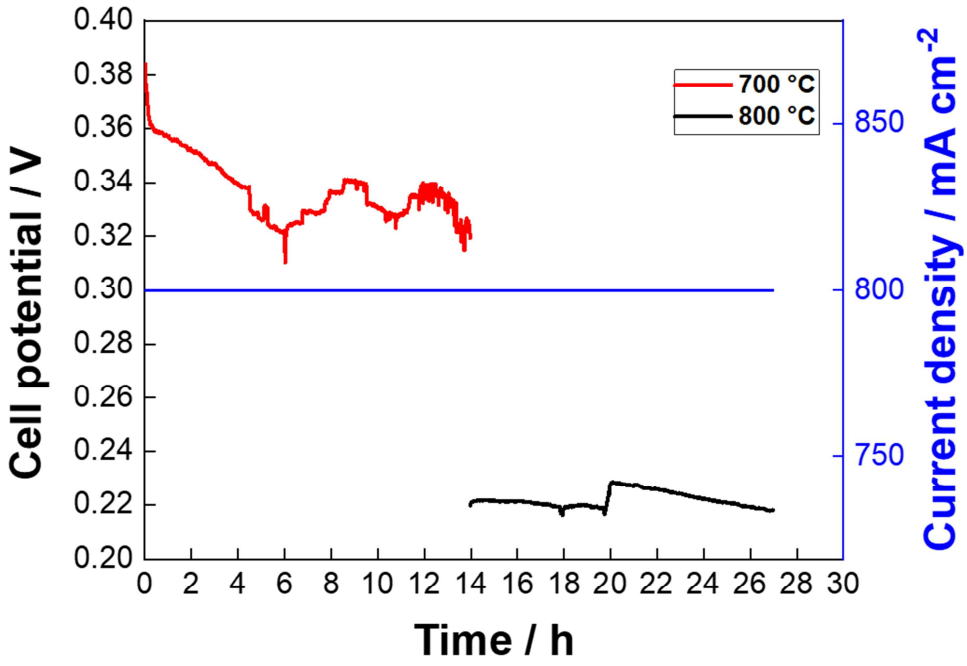

Figure 3. A galvanostatic test carried out between 700 and 800 °C.

A number of diagnostic tests were executed during the galvanostatic evaluations, including impedance spectroscopy (EIS) and polarization curves (I-V curves). As shown in figure 4, the EIS spectra were obtained at 700 °C and 800 °C. As expected, with increasing temperature, the series resistance (Rs), given by the intercept of the spectrum at high frequency with the x-axis, decreased from 0.45 ohm cm^2 at 700°C to 0.25 ohm cm^2 at 800 °C. The total resistance (Rt) of the cell decreased in response to the highest temperature investigated (given by the intercept between the low frequency spectrum and the x-axis). A value of approximately 0.28 ohm cm^2 was recorded for Rt at 800 °C, while the Rt was about 0.5 ohm cm^2 at 700 °C. A highly overlapped pair of semicircles approximately represents the characteristic spectrum in both cases, with each one representing the mechanisms occurring at each electrode. In this way, the high overlapping behaviour of these semicircles could indicate that the reduction of H_2O and the oxidation of ethanol have relatively similar kinetics. In contrast, both experiments were significantly affected by the series resistance, which is generally caused by the electrolyte resistance. These experiments were conducted using an electrolyte supported cell (ESL) design as explained in the experimental part. At the high temperatures investigated, thin film electrodes with mixed ionic-electronic conductivity (MIEC) contributed only a small amount to the series resistance. In contrast, the electrolyte thickness was 300 microns, and as a result, the path to be crossed by the oxygen ions from the anode where they were formed to the cathode where they were combined with ethanol was relatively lengthy, even if the electrolyte had excellent conductivity and oxygen ions mobility. With this in mind, it is possible to predict very high current densities for a cell architecture with a thin layer electrolyte, such as that used in anode supporting cells (ASC).

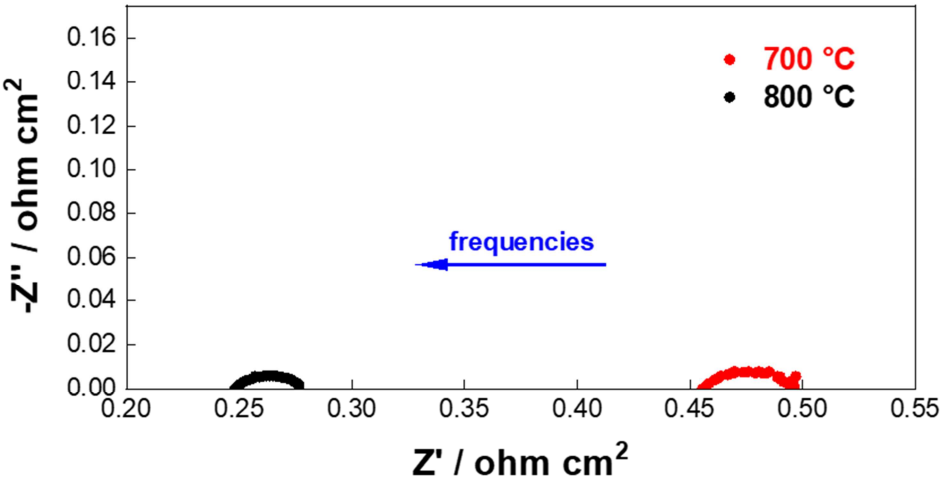

Figure 4. Comparison of the EIS spectrum at 700°C and 800°C.

The polarization curves obtained at 700 and 800 °C for this experimental cell are shown in figure 5. There is only a limited activation constraint at 700 °C at very low current densities; after that, ohmic limitations dominate cell performance. At 800 °C, the activation control was almost nonexistent and the only constraint on the cell performance was the ohmic resistance, which was in large part due to the electrolyte. There were no significant diffusion problems in either experiment.

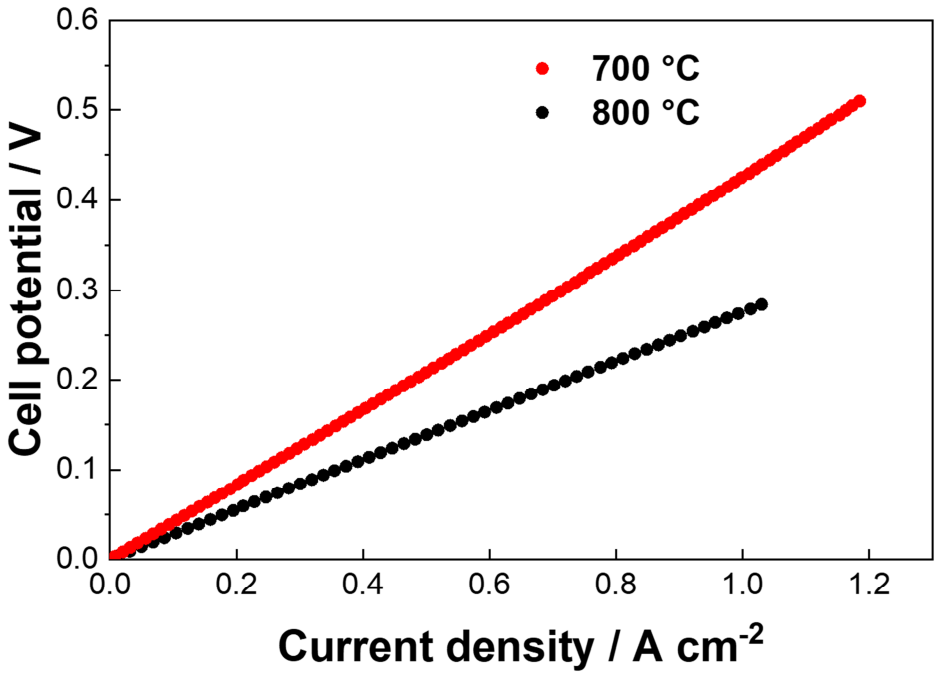

Figure 5. Comparison of the I-V curves measured at 700°C and 800°C.

Figure 6 shows the results of a preliminary XPS analysis of the electrocatalyst surface on both electrodes. Since we analyzed fragments of cells discharged from a test requiring sealing with ceramic paste, these analyses produced very complex survey spectra. We also used gold paste to ensure proper electrical contacts. These factors contributed to the complexity of the spectra collected. The anode side of the cell showed a peak due to the presence of Na. Clearly, this was caused by the nature of the ethanol used. Ethanol sold

in Brazil is made from sugarcane and contains traces of Na derived from NaOH used during manufacturing. Another apparent intensified peak was that caused by carbon species present on the anode surface.

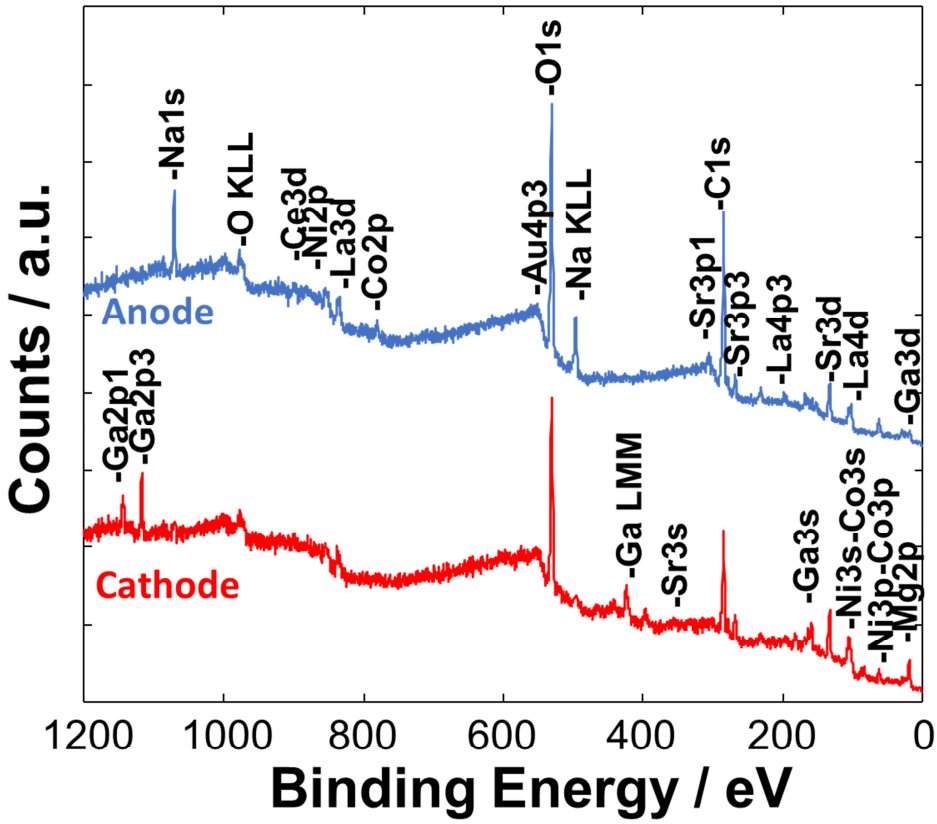

Figure 6. A XPS survey of the cathode and anode of the spent cell.

Conclusions

As of now, further analyses are underway to assess the potential of this electrochemical process. At this point, it can be concluded that H_2O electrolysis can be carried out differently than the conventional methods by adopting an electrochemical ceramic cell, such as the SOFC/SOEC which can use different renewable resources including those derived from biomasses. A solution such as this could solve at once two common problems of green H2 generation, namely the fluctuation of solar and wind power, which requires a backup electrical system, and the capex costs of power generators. There is of course room for further optimization if a novel proton-conducting electrolyte is used for electrochemical reforming, but it deserves to be investigated in greater detail using conventional oxygen ion conductors as electrolytes as well. This paper describes preliminary experiments carried out with a fully perovskite cell that may solve the typical issues associated with the materials used in commercial cells. Despite the excellent results in this study, there are several other aspects yet to be evaluated, including the stability and the faradaic efficiency of this process, which is currently under estimation. In spite of this, the preliminary results appeared to be very promising.

Acknowledgments

The authors affiliated with IQSC-USP thanks the Fapesp/Shell project Proc 2020/15230-5 - BG E&P Brasil (Shell)-CPE "Research Centre for Greenhouse Gas Innovation - RCG2I"

All authors acknowledge ITELECTROLAB, the joint lab between CNR-ITAE and IQSC-USP financed by the National Research Council of Italy and the bilateral project "FlexPower- Solid Oxide Fuel Cell fed with Biofuel as an Electric Flexible Provider in a Distributed Grid" granted by MAECI-FAPESP.

References

1. H. Ritchie, Sector by sector: where do global greenhouse gas emissions come from?, in, https://ourworldindata.org/ghg-emissions-by-sector (2020).
2. M. Lo Faro, O. Barbera and G. Giacoppo, in *Hybrid Technologies for Power Generation*, M. Lo Faro, O. Barbera and G. Giacoppo Editors, p. xvii, Academic Press (2022).
3. M. Lo Faro, S. Trocino, S. C. Zignani, V. Antonucci and A. S. Aricò, *International Journal of Hydrogen Energy*, **42**, 27859 (2017).
4. S. H. Jensen, P. H. Larsen and M. Mogensen, *International Journal of Hydrogen Energy*, **32**, 3253 (2007).
5. M. Lo Faro, W. Oliveira da Silva, W. V. Barrientos, G. G. A. Saglietti, S. C. Zignani, V. Antonucci, E. A. Ticianelli and A. S. Aricò, *International Journal of Hydrogen Energy*, **45**, 5134 (2020).
6. M. Lo Faro, R. M. Reis, G. G. A. Saglietti, V. L. Oliveira, S. C. Zignani, S. Trocino, S. Maisano, E. A. Ticianelli, N. Hodnik, F. Ruiz-Zepeda and A. S. Aricò, *Applied Catalysis B: Environmental*, **220**, 98 (2018).
7. F. Liu, T. Wang, J. Li, T. Wei, Z. Ye, D. Dong, B. Chen, Y. Ling and Z. Shao, *Chemical Engineering Journal*, **434**, 134699 (2022).
8. M. Lo Faro, D. A. Cantane and F. Naro, *International Journal of Hydrogen Energy* (2022).
9. S. C. Singhal, *Solid State Ionics*, **135**, 305 (2000).
10. S. Vecino-Mantilla, E. Quintero, C. Fonseca, G. H. Gauthier and P. Gauthier-Maradei, *ChemCatChem*, **12**, 1453 (2020).
11. M. Lo Faro and A. S. Arico, in *Membranes for Clean and Renewable Power Applications*, A. Gugliuzza and A. Basile Editors, p. 237, Woodhead Publ Ltd, Cambridge (2014).
12. S. Trocino, M. Lo Faro, S. C. Zignani, V. Antonucci and A. S. Aricò, *Applied Energy*, **233-234**, 386 (2019).
13. M. Lo Faro and A. S. Arico, *International Journal of Hydrogen Energy*, **38**, 14773 (2013).